

T. KAWABATA\*, T. NAMIKI\*, K. MATSUDA\*, D. TOKAI\*, S. MURAKAMI\*, K. NISHIMURA\*

## SUPERCONDUCTIVITY OF $MgB_2$ COMPOSITED WITH Mg-Zn ALLOYS

### NADPRZEWODNICTWO KOMPOZYTÓW $MgB_2$ – STOP Mg-Zn

The three-dimensional penetration method combined with semi-solid casting was used to fabricate metal-powder composite superconducting materials of  $MgB_2$  with magnesium alloys:  $MgB_2/Mg - xwt\% Zn$  ( $x = 1, 3, 6, 9$ ). X-ray diffraction measurements indicated predominant peak patterns of  $MgB_2$  and a host alloy. Measured electrical resistivity ( $\rho$ ) versus temperature showed a clear signal of superconducting transition at about 34 K for all the samples cut out from the composites. External field ( $H$ ) dependence of  $\rho(T, H)$  provided upper critical field of about 5 T. A volume fraction of the superconducting state of the sample estimated from a low external field part of magnetization was almost the same as the nominal ratio of  $MgB_2$  powder against the host material. A magnetic hysteresis loop observed at 5 K suggested that an addition of Zn element to magnesium host-matrix little changed the critical current density ( $J_c$ ). A comparison of the present results with the previous ones of  $MgB_2/Mg-Al-Zn$  systems confirmed that simultaneously doped Al and Zn were necessary to enhance  $J_c$ . Specific heat measurements of the sample with an external field showed that the bulk superconductivity of  $MgB_2$  was well conserved in the composites.

*Keywords:*  $MgB_2$ , composite materials, magnesium alloy, specific heat

Metodę trójwymiarowego zagęszczania w połączeniu z odlewaniem w stanie stało-ciekłym użyto do wytworzenia kompozytowych materiałów nadprzewodzących proszku  $MgB_2$  ze stopami magnezu  $MgB_2/Mg - x \% \text{ wag Zn}$  ( $x = 1, 3, 6, 9$ ). Rentgenowskie pomiary dyfrakcyjne wykazały obecność wyraźnych pików od  $MgB_2$  i osnowy. Oporność elektryczna ( $\rho$ ) mierzona w zależności od temperatury zawierała wyraźny sygnał przejścia nadprzewodzącego około 34 K dla wszystkich próbek wyciętych z kompozytów. Zależność  $\rho(T, H)$  od zewnętrznego pola ( $H$ ) pokazała górną krytyczną wartość pola 5 T. Udział objętościowy próbki w stanie nadprzewodzącym oszacowany z niskiej części zewnętrznego pola magnetyzacji był prawie taki sam jak stosunek nominalnej zawartości proszku  $MgB_2$  do materiału osnowy. Pętla histerezy magnetycznej obserwowana przy 5 K sugeruje, że dodatek Zn do osnowy magnezowej niewiele zmienia gęstość prądu krytycznego ( $J_c$ ). Porównanie obecnych wyników z wcześniej uzyskanymi dla układów  $MgB_2/Mg-Al-Zn$  potwierdziło, że do zwiększenia  $J_c$  konieczne jest jednoczesne domieszkowanie Al i Zn. Pomiary ciepła właściwego próbki w zewnętrznym polu wykazały, że nadprzewodnictwo  $MgB_2$  zostało dobrze zachowane w kompozytach.

### 1. Introduction

Attractive points of superconducting properties of  $MgB_2$  are high critical temperature ( $T_c$ ) [1] among metallic compounds, relatively large upper critical field [2], isotropic transport properties against the crystallographic directions [3], and rather long coherence length [4], which stimulate plenty of research activities to develop suitable processes for producing  $MgB_2$  wires and tapes [5, 6]. For practical use, the critical current density ( $J_c$ ) of  $MgB_2$  has been one of major issues of research; a well known problem is that  $J_c$  drops rapidly with increasing magnetic field due to its poor flux pinning. Improvements in  $J_c$  (enhancements of flux pinning) were achieved by various approaches; doping by chemical compounds [7], substitution of Mg and/or B by other elements [8, 9], high-pressure application during process [10], various heat-treatment [11], etc. Theoretical studies for variations of

the band structure by element substitution were also carried out [12-14]. The consistent interpretation for  $J_c$  variations with fabrication processes has been given via the comprehensive studies of normal-state resistivity of  $MgB_2$  by Yamamoto et al [15-17], using  $MgB_2$  bulk samples with systematically varied packing factors (density).

The three-dimensional penetration method combined with semi-solid casting (SS-3DPC) has been successfully used to fabricate metal-powder composite superconducting materials [18]. This is a kind of the ex-situ technique, in which a half-melted host metal, such aluminum or magnesium, penetrated  $MgB_2$  powder-preform by pressure. A low temperature casting is a great advantage of SS-3DPC compared the powder-in-tube (PIT) method [19], in which high temperature heat treatments easily introduced large voids in  $MgB_2$  grains. Our previous work on  $MgB_2/Al$  composite materials demonstrated that the superconducting transition tempera-

\* GRADUATE SCHOOL OF SCIENCE AND ENGINEERING, UNIVERSITY OF TOYAMA, 3190, GOFUKU, TOYAMA, 930-8555, JAPAN

ture ( $T_c$ ) was observed at 38 K on the resistivity, a superconducting volume fraction estimated from magnetization was about 50% [18], and further a superconducting wire of  $MgB_2/Al$  of 1mm diameter was extruded [20]. Experimental results of  $MgB_2$ -powder composite materials with the magnesium-aluminum-zinc alloys prepared by the SS-3DPC technique have been given elsewhere [21], which elucidated that doping Al and Zn elements enhanced  $J_c$ . This result facilitates a study of the  $MgB_2/Mg$ -Zn system to investigate if the enhancement of  $J_c$  originated in doped Zn, since Zn has been known to increase  $T_c$  of  $MgB_2$  [22]. This paper deals with the  $MgB_2$  composited samples with host materials of  $Mg$ - $x$  wt% Zn ( $x = 1, 3, 6, 9$ , hereafter noted as Z1, Z3, Z6, Z9, respectively). The results are compared with our previous ones of  $MgB_2/Mg$  (noted as M0) and  $MgB_2/Mg$ -9wt%Al-1%Zn (AZ91) samples [21].

## 2. Experimental

$MgB_2$  powders provided from Kojundo Chemical Laboratory have a purity of more than 99%, and an averaged grain-size was approximately 40  $\mu m$ . The details of sample preparation have been given elsewhere [18, 21]. A conventional scanning electron microscope (SEM) was used to inspect the  $MgB_2$  powders and host materials in the composites. Figure 1 illustrates a typical SEM image at a cut surface of the obtained billet of  $MgB_2/Mg$ -9wt%Zn. It is clear that the magnesium host metal (gray-white area) tightly bound  $MgB_2$  particles (dark-gray shape). A density of the central part of the billet was about 2.1  $g/cm^3$ , which is in between those of 1.74  $g/cm^3$  for Mg and 2.62  $g/cm^3$  for  $MgB_2$ . The crystal structure of  $MgB_2$  composite material was analyzed by the Cu  $K\alpha$  x-ray diffraction measurements. Resistivity and specific heat measurements were carried out in the range from 2 to 300 K using the physical property measurement system (PPMS, Quantum Design Co. Inc.). Magnetization data were accumulated by a SQUID magnetometer (MPMS, Quantum Design Co. Inc.) in the same temperature range.

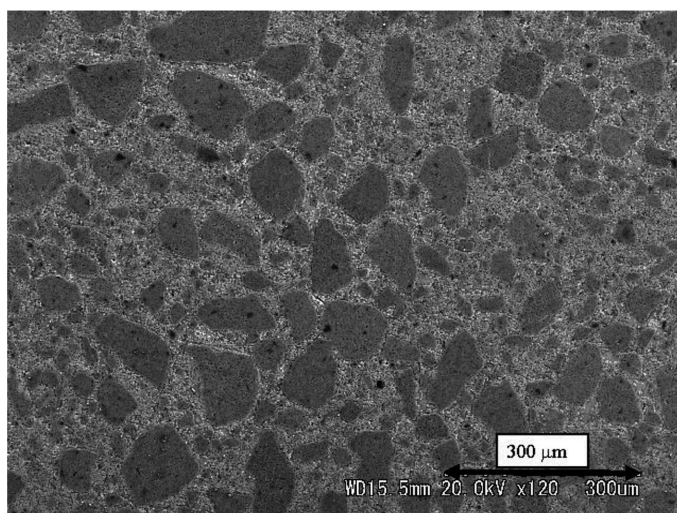


Fig. 1. SEM image at a cut surface of the  $MgB_2/Mg$ -9wt%Zn composite sample

## 3. Results and discussion

Figure 2 shows XRD patterns of the present samples together with the previous data of  $MgB_2/Mg$ -9wt%Al-1wt% Zn [21] for a comparison. The peaks of  $MgB_2$ -phase (marked with open circle) and Mg (closed circle) were observed. There are unknown peaks near 36 and 40 degrees with the AZ91 sample. In our previous paper [21] we speculated them as peaks from Mg-Zn alloys and ZnO referring other literature [9, 22]. A detailed investigation, however, indicated that the peaks are likely due to the  $Mg_{17}Al_{12}$  precipitation. Doping Zn to Mg-Al alloys reduced the solid solubility of Al in Mg, resulting in precipitation of  $Mg_{17}Al_{12}$  [23]. The lattice parameters of  $MgB_2$  were found to change little with Zn contents, e.g.  $a = 0.3091$  nm and  $c = 0.3532$  nm with Z1 sample and  $a = 0.3089$  nm and  $c = 0.3528$  nm with Z6 sample.

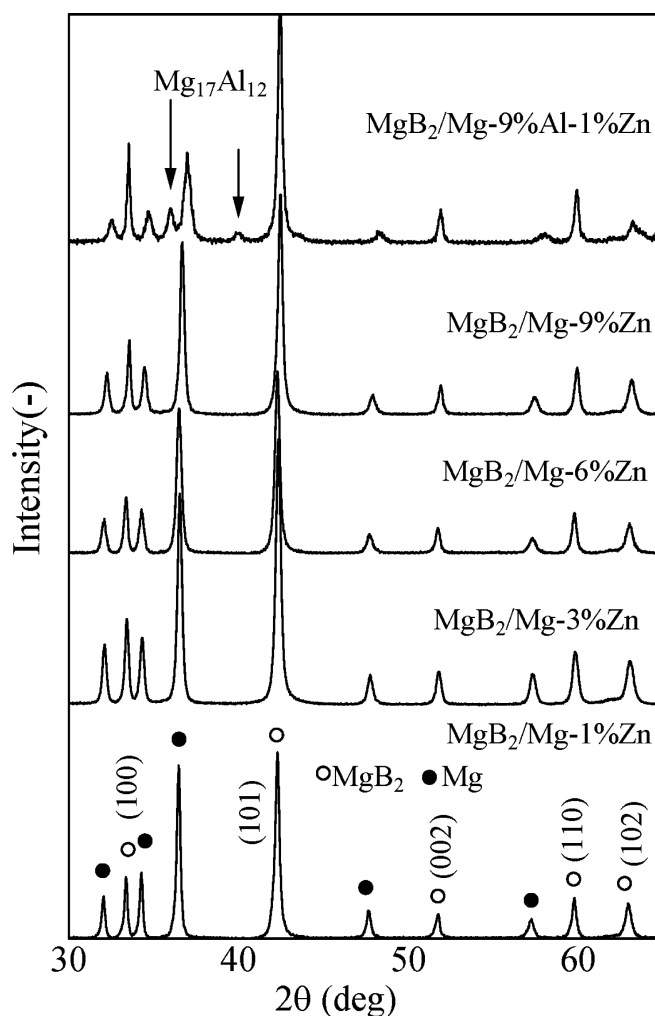


Fig. 2. The x-ray powder diffraction pattern of  $MgB_2$  with Mg-Zn and Mg-9wt%Al-1wt%Zn [21]

Low temperature parts of the electrical resistivity data were shown in Fig. 3. The  $T_c$  value estimated as an average of  $T_c$  (on set) and  $T_c$  (off set) and the residual resistivity ( $\rho_0$ ) as an average of those around 40 K are listed in Table 1, in which the results of M0 and AZ91 samples are quoted from the previous work [21]. Comparing the present results of  $T_c$  and  $\rho_0$  with those of  $MgB_2/Mg$ -Al-Zn system, the  $T_c$  and  $\rho_0$  variations with Z1 – Z9 samples are surprisingly small;

i.e. the doped Al element brought about a significant effect on the electron conductivity. The substitution of Al for Mg in  $\text{MgB}_2$  has been considered to fill the electronic state and decrease the density of state at the Fermi level, leading to the decrease of  $T_c$  [24]. Although, in the SS-3DPC process, the  $\text{MgB}_2$  particles were seen to keep their shape, doped Al most likely diffused into the  $\text{MgB}_2$  particles and partly substituted Mg sites and made precipitations, which disturbed electron conductivity and coherence of electron pairs.

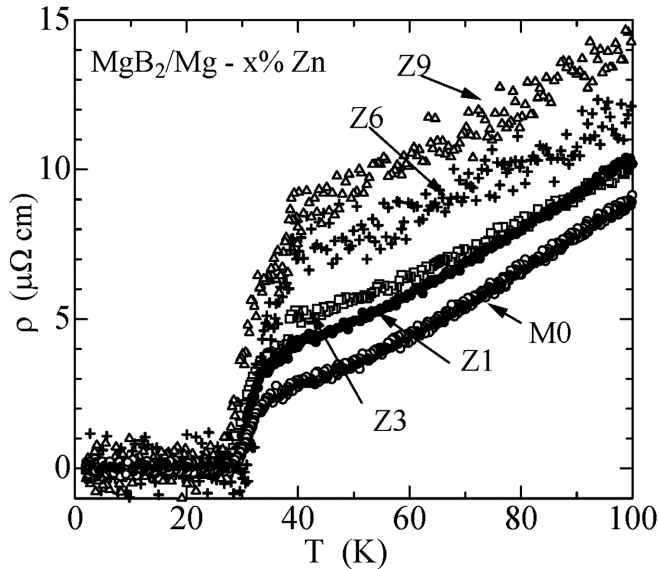


Fig. 3. Temperature dependence of resistivity of  $\text{MgB}_2/\text{Mg} - x\% \text{ Zn}$  ( $x = 0 - 9$ , below 100 K)

TABLE 1

Host material, abbreviate letter for the sample, critical temperature estimated from  $\rho$ , residual resistivity  $\rho_0$  around 40 K, upper critical field estimated from  $\rho(T, H)$ , superconducting volume fraction at 5 K, lower critical field at 5 K, critical current density at 1 T and 5 K

host material	label	$T_c$ K	$\rho_0$ $\mu\Omega\text{cm}$	$H_{c2}(0)$ T	vol. %	$H_{c1}$ mT	$J_c$ kA/cm <sup>2</sup>
Mg*	M0	33.7	2.9	–	65	50	5.3
Mg+1%Zn	Z1	33.1	4.2	5.2	48	37	3.8
Mg+3%Zn	Z3	32.5	5.2	4.4	46	42	5.2
Mg+6%Zn	Z6	34.6	7.6	6.8	53	48	4.8
Mg+9%Zn	Z9	33.2	8.6	5.2	54	47	5.6
Mg+9%Al+1%Zn*	AZ91	26.4	36.9	–	56	54	15.8

\* These results were quoted and estimated from the data in ref. [21]

The temperature dependence of resistivity at several externally applied fields was measured for the Z1 – Z9 samples. The normalized resistivity  $\rho(T, H)/\rho_0$  using the  $\rho_0$  values listed in Table 1 for Z1 sample is shown in Fig. 4. The upper critical field  $H_{c2}$  was determined from the offset points of the transition temperature in the  $\rho(T, H)/\rho_0$  curve. The temperature dependence of  $H_{c2}(T)$  are shown in Fig. 5, which indicates that  $H_{c2}$  varies almost linearly with  $T$ . Extrapolation to  $T = 0$  K with a linear fit of the data points for each sample results in the values of  $H_{c2}(0)$  in Table 1. The deduced  $H_{c2}(0)$  values are

a little related with the observed  $T_c$  values, but rather smaller than the reported values for bulk  $\text{MgB}_2$  samples: e.g. for a single crystal with field along the c-plane,  $H_{c2}(0) = 14.5$  T and field along the c-axis,  $H_{c2}(0) = 3.2$  T [25].

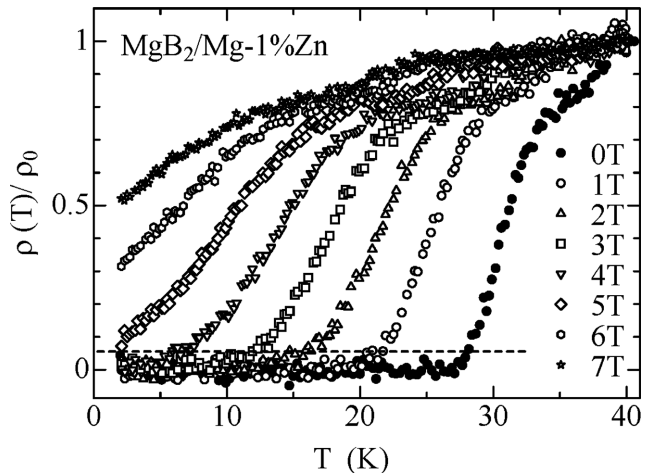


Fig. 4. Temperature dependence of normalized electrical resistivity  $\rho(T, H)/\rho_0$  under several external fields for  $\text{MgB}_2/\text{Mg} - 1\% \text{ Zn}$

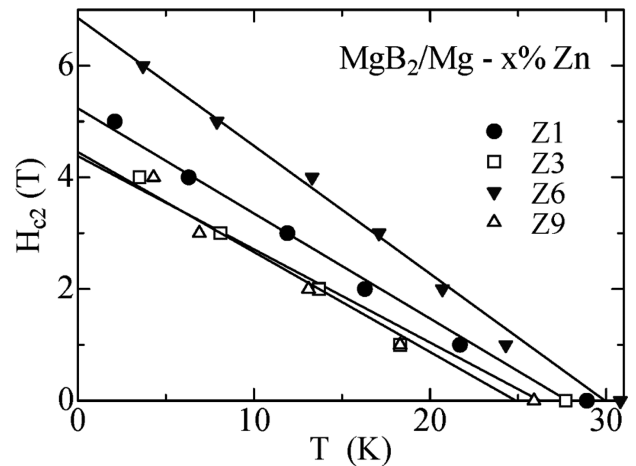


Fig. 5. Temperature dependence of upper critical field for  $\text{MgB}_2/\text{Mg} - x\% \text{ Zn}$

The hysteresis loops of magnetizations are shown in Fig. 6. There is little obvious change in magnitude of the magnetization with doping Zn element. (The data points with M0 and Z1 – Z9 almost overlapped each other, but those of AZ91 are apparently larger than the others) The volume fractions of the superconducting part of the samples and the lower critical field  $H_{c1}$  at 5 K were estimated from the initial  $M-H$  data points below 0.2 T. A  $H_{c1}$  value for certain  $x$  was taken as the field at which  $M(H)$  curve deviates from the linear relation expected for the perfect diamagnetism, and the slope value provides the volume fraction, which is almost the same as the nominal value of  $\text{MgB}_2$  powder against the host material. This result implies that the host materials banded  $\text{MgB}_2$  particles without melting them. The  $M-H$  loop curves also imply that doping Zn element did not enhance  $J_c$  since  $J_c$  linearly depends on the amplitude of the magnetization difference at a given field. The critical current density  $J_c(H)$  of the samples (listed in Table 1) were evaluated using the equation of an extended Bean critical state model [26, 27] of

$J_c(H) = 20\Delta M / a(1 - a/3b)$ , where  $\Delta M$  is the amplitude of the  $M$ - $H$  curve in  $\text{emu}/\text{cm}^3$  at given field and temperature, and  $a$  and  $b$  are the sample length and width, respectively. This result quite contrasts to that of  $\text{MgB}_2/\text{Mg-Al-Zn}$  system, in which the simultaneously doped Al and Zn elements increased  $J_c$ . This fact suggests that the  $J_c$  enhancement observed in  $\text{MgB}_2/\text{Mg-Al-Zn}$  system is predominantly ascribed to substitution of Al for Mg and precipitation of  $\text{Mg}_{17}\text{Al}_{12}$  (observed x-ray diffraction) stimulated by Zn addition.

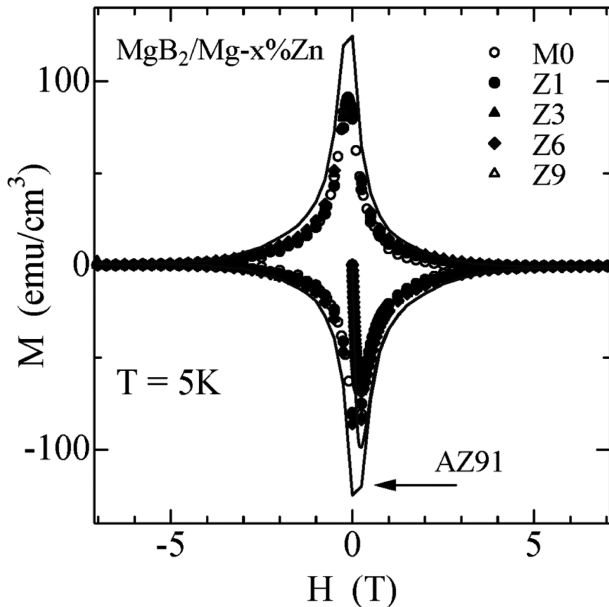


Fig. 6.  $M$ - $H$  hysteresis loops for  $\text{MgB}_2/\text{Mg} - x\%$  Zn at 5 K

Resistivity and magnetization often give misleading information on the bulk superconducting property. Resistivity is sensitive to the first percolation path, but no information can be extracted below  $T_c$ . Magnetization is sensitive to shielding by a superconducting superficial layer, so a precise calculation of the demagnetization factor is required to estimate a superconducting volume fraction. Specific heat measurements, in contrast, provide information on the bulk property. The specific heat jump is directly proportional to the superconducting volume, and its shape mirrors the distribution of  $T_c$ . Figure 7 presents an experimental result of specific heat measurement for the Z6 sample of 22.26 mg.

The measurements were carried out without field (data points were marked by closed circle) and then, with a field of 7 T (open circle) in Fig. 7(a) by the  $C/T$  versus  $T^2$  scale. The specific heat jump due to the superconducting phase transition is noticeable. We estimate the specific heat difference between the superconducting and normal states ( $\Delta C = C(0\text{T}) - C(7\text{T})$ ) as shown in Fig. 7(b). The  $\Delta C/T$  variation against temperature surprisingly resembles to those in literature for pure  $\text{MgB}_2$  [28, 29]. The calculated  $\Delta C/T_c$  value in Fig. 7(b) is  $0.035\text{mJ/g K}^2$ , which is about 55 % of a typical reported one of  $3.0\text{mJ/mol K}^2 (= 0.065\text{mJ/g K}^2)$  for pure  $\text{MgB}_2$  [29]. This value of the superconducting volume fraction is almost the same as that obtained from the  $M$ - $H$  data (see Table 1), supporting our data analysis with  $M$ - $H$  data. The observed broad peak of  $\Delta C/T$  has been associated with the two-band gap for  $\text{MgB}_2$  electronic structure [28]. The specific heat curves in superconducting and normal states intersect at the temperature of  $0.52T_c$  for a

weak-coupling superconductor [30]; this is definitely observed in the present sample.

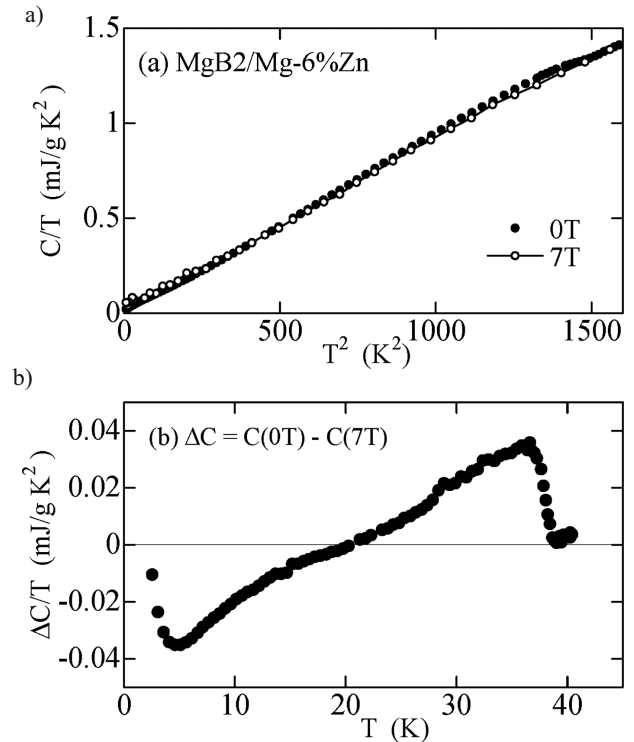


Fig. 7. (a) Specific heat of  $\text{MgB}_2/\text{Mg-6\%Zn}$  sample with zero field (closed circle) and a field of 7 T (open circle) in  $C/T$ - $T^2$  scale. (b) The specific heat difference between the superconducting  $C(0\text{T})$  and normal  $C(7\text{T})$  states estimated from the data (a)

#### 4. Conclusion

The present experimental work demonstrates that the three-dimensional penetration method combined with semi-solid casting is a suitable process to fabricate  $\text{MgB}_2$  powder-magnesium-zinc alloys composite materials. The observed superconducting properties, such  $T_c$ ,  $J_c$ , and  $\Delta C$ , are comparable to those of pure  $\text{MgB}_2$  bulk sample. Doping Zn element to  $\text{MgB}_2/\text{Mg}$  composites little enhanced  $J_c$ , being different from the results observed in  $\text{MgB}_2/\text{Mg-Al-Zn}$  system. The present results confirm that doped Al to  $\text{MgB}_2/\text{Mg}$  composite raised a predominant effect on the  $J_c$  enhancement due to substitution for Mg, and doped Zn brought about an additional effect on the  $J_c$  enhancement by stimulating precipitation of  $\text{Mg}_{17}\text{Al}_{12}$  which could work as a pinning center.

#### Acknowledgements

This study was partially supported by the Japan Society for the Promotion of Science (No. 22360313).

#### REFERENCES

- [1] J. Nagamatsu, N. Nakagawa, T. Muranaka, Y. Zenitani, J. Akimistu, Nature **410**, 63 (2001).
- [2] V. Braccini et al. Phys. Rev. **B71**, 012504 (2005).

- [3] T. Masui, S. Lee, A. Yamamoto, S. Tajima, *Physica* **C378-381**, 216 (2002).
- [4] T. Klein, L. Lyard, J. Marcus, Z. Holanová, C. Marcenat, *Phys. Rev.* **B73**, 184513 (2006).
- [5] K. Tanaka, M. Okada, M. Hirakawa, H. Yamada, H. Kumakura, H. Kitaguchi, *Supercond. Sci. Technol.* **18**, 678 (2005).
- [6] K. Tanaka, K. Funaki, T. Sueyoshi, Y. Sasashige, K. Kajikawa, M. Okada, H. Kumakura, H. Hayashi, *Supercond. Sci. Technol.* **21**, 095007 (2008).
- [7] E.W. Collings, M.D. Sumption, M. Bhatia, M.A. Susner, S.D. Bohnenstiehl, *Supercond. Sci. Technol.* **2**, 1030011 (2008).
- [8] W.K. Yeoh, S.X. Dou, *Physica* **C456**, 170 (2007).
- [9] P. Toulemonde, N. Musolino, H.L. Suo, R. Flukiger, *J. Supercond.* **15**, 613 (2002).
- [10] P. Toulemonde, N. Musolino, R. Flukiger, *Supercond. Sci. Technol.* **16**, 231 (2003).
- [11] S. Soltanian, X.L. Wang, J. Horvat, S.X. Dou, M.D. Sumption, M. Bhatia, E.W. Collings, P. Munroe, M. Tomsic, *Supercond. Sci. Technol.* **18**, 658 (2005).
- [12] P.P. Singh, P.J.T. Joseph, *J. Phys. Condens. Matter* **14**, 12441 (2002).
- [13] P.P. Singh, *Bull. Matter. Sci.* **26**, 131 (2003).
- [14] P.P. Singh, *Solid State Comm.* **127**, 271 (2003).
- [15] J.M. Rowell, *Supercond. Sci. Technol.* **16**, R17 (2003).
- [16] A. Yamamoto, J. Shimoyama, K. Kishio, T. Matsushita, *Supercond. Sci. Technol.* **20**, 658 (2007).
- [17] T. Matsushita, M. Kiuchi, A. Yamamoto, J. Shimoyama, K. Kishio, *Supercond. Sci. Technol.* **21**, 015008 (2008).
- [18] K. Matsuda, T. Saeki, K. Nishimura, S. Ikeno, Y. Yabumoto, K. Mori, *Materials Transactions* **47**, 1214 (2006).
- [19] S.X. Dou, X.L. Wang, J. Horvat, D. Milliken, A.H. Li, K. Konstantinov, E.W. Collings, M.D. Sumption, H.K. Liu, *Physica* **C361**, 79 (2001).
- [20] K. Matsuda, K. Nishimura, S. Ikeno, K. Mori, S. Aoyama, Y. Yabumoto, Y. Hishinuma, I. Mullerova, L. Frank, V.V. Yurchenko, T.H. Johansen, *J. Phys. Conf. Series* **97**, 012230 (2008).
- [21] Y. Shimizu, K. Matsuda, M. Mizutani, K. Nishimura, T. Kawabata, S. Ikeno, Y. Hishinuma, S. Aoyama, *Materials Transactions* **52**, 272 (2011).
- [22] Y. Kimishima, Y. Sugiyama, S. Numa, M. Uehara, T. Kuramoto, *Physica* **C468**, 1185-1187 (2008).
- [23] S. Celotto, *Acta mater.* **48**, 1775 (2000).
- [24] J.S. Slusky, N. Rogado, K.A. Regan, M.A. Hayward, P. Khalifah, T. He, K. Inumaru, S.M. Loureiro, M.K. Haas, H.W. Zandbergen, R.J. Cava, *Nature* **410**, 343-345 (2001).
- [25] M. Zehetmayer, M. Eisterer, J. Jun, S.M. Kazakov, J. Karpinski, A. Wisniewski, H.W. Weber, *Phys. Rev.* **B66**, 052505 (2002).
- [26] C.P. Bean, *Phys. Rev. Lett.* **8**, 250 (1962).
- [27] Z. Cheng, B. Shen, J. Zhang, S. Zhang, T. Zhao, H. Zhao, *J. Appl. Phys.* **91**, 7125 (2002).
- [28] H.J. Choi, D. Roundy, H. Sun, M.L. Cohen, S.G. Louie, *Nature* **418**, 758-760 (2002).
- [29] H.D. Yang, J.-Y. Lin, H.H. Li, F.H. Hsu, C.J. Liu, S.-C. Li, R.-C. Yu, C.-Q. Jin, *Phys. Rev. Lett.* **87**, 167003 (2001).
- [30] Y. Wang, T. Plackowski, A. Junod, *Physica* **C355**, 179 (2001).